MOLECULAR AND CELLULAR BIOLOGY, Mar. 2005, p. 1696–1712 Vol. 25, No. 5
0270-7306/05/$08.00+0 doi:10.1128/MCB.25.5.1696–1712.2005

Epithelium-Mesenchyme Interactions Control the Activity of Peroxisome Proliferator-Activated Receptor β/δ during Hair Follicle Development

Nicolas Di-Poï,[1] Chuan Young Ng,[1] Nguan Soon Tan,[1] Zhongzhou Yang,[2] Brian A. Hemmings,[2] Béatrice Desvergne,[1] Liliane Michalik,[1] and Walter Wahli[1]*

Center for Integrative Genomics, NCCR Frontiers in Genetics, University of Lausanne, Lausanne,[1] and Friedrich Miescher Institute for Biomedical Research, Basel,[2] Switzerland

Received 26 July 2004/Returned for modification 26 August 2004/Accepted 18 November 2004

Hair follicle morphogenesis depends on a delicate balance between cell proliferation and apoptosis, which involves epithelium-mesenchyme interactions. We show that peroxisome proliferator-activated receptor beta/delta (PPARβ/δ) and Akt1 are highly expressed in follicular keratinocytes throughout hair follicle development. Interestingly, PPARβ/δ- and Akt1-deficient mice exhibit similar retardation of postnatal hair follicle morphogenesis, particularly at the hair peg stage, revealing a new important function for both factors in the growth of early hair follicles. We demonstrate that a time-regulated activation of the PPARβ/δ protein in follicular keratinocytes involves the up-regulation of the cyclooxygenase 2 enzyme by a mesenchymal paracrine factor, the hepatocyte growth factor. Subsequent PPARβ/δ-mediated temporal activation of the antiapoptotic Akt1 pathway in vivo protects keratinocytes from hair pegs against apoptosis, which is required for normal hair follicle development. Together, these results demonstrate that epithelium-mesenchyme interactions in the skin regulate the activity of PPARβ/δ during hair follicle development via the control of ligand production and provide important new insights into the molecular biology of hair growth.

Hair follicles (HFs) are cutaneous appendages exerting many important functions in mammals, including thermoregulation, skin protection, and social interaction. Like tooth and feather development, HF morphogenesis is governed by complex bidirectional epithelium-mesenchyme interactions between epithelial keratinocytes and underlying dermal cells of the mesenchymal condensations. In particular, early developmental steps involve three signals that lead to (i) the thickening of the epithelial surface (first dermal signal), (ii) the formation of the dermal papilla (first epithelial signal), and (iii) the downgrowth of follicular epithelial cells (hair peg) into the dermis (second dermal signal) (31). The whole process of HF development has been divided into eight consecutive stages, which tightly depend on the balance in keratinocytes between apoptosis and proliferation (27). Once formed, HFs continuously cycle through periods of intensive growth (anagen), apoptosis-driven regression (catagen), and resting (telogen).

Although the molecular nature of the inductive signals that underlie the formation of the HF is largely unknown, distinct signaling molecules, such as β-catenin, T-cell factor (TCF), Sonic hedgehog (SHH), and hepatocyte growth factor (HGF), have been implicated at various stages of HF development (31). In addition, many members of the nuclear receptor family, including the estrogen (NR3A), vitamin D (NR1I), and retinoid receptors (NR1B and NR2B), have been identified as important modulators of skin as well as HF development and homeostasis, both in humans and mice (1, 23). Recent reports also suggest a role for peroxisome proliferator-activated receptor (PPAR) in fetal epidermal development, particularly keratinocyte and sebocyte differentiation in rodents (5, 29, 39).

The subfamily of PPARs comprises three isotypes, PPARα (NR1C1), PPARβ/δ (NR1C2; called PPARβ below), and PPARγ (NR1C3), that regulate gene transcription upon ligand-induced activation (hypolipidemic drugs, polyunsaturated fatty acids, or cyclooxygenase [COX]-derived prostaglandins) and heterodimerization with the retinoid X receptor (RXR) (NR2B) (9). Each PPAR exhibits a specific tissue distribution and performs distinct roles in lipid metabolism, inflammation, diabetes, and cancer (20, 30). We have shown previously that all three PPAR isotypes, and predominantly PPARβ, are expressed in the differentiating epidermis and HFs during embryonic skin development in rats and mice (5, 29). Interestingly, PPAR expression specifically disappears from the interfollicular epidermis after birth and becomes undetectable in the adult, whereas it remains highly expressed in postnatal and adult HFs (29). The expression and activation of PPARβ is rapidly stimulated in the adult interfollicular epidermis by inflammatory stimuli like tumor necrosis factor alpha during skin injury (41). In accordance, delayed wound closure was observed in PPARβ-mutant female mice, largely due to an altered balance between proliferation and apoptosis as well as to defects in cell adhesion and migration of PPARβ-mutant keratinocytes (10, 29).

The specific expression of PPARβ in the differentiating HF already from the early embryonic stages pointed to a possible role of PPARβ in the control of HF development. In favor of this, PPAR ligands were already reported to increase the survival of human HFs in culture (3). In addition, we previously demonstrated that PPARβ activates the Akt signaling pathway in keratinocytes (11), which was recently shown to affect hair

* Corresponding author. Mailing address: Center for Integrative Genomics, Biology Building, University of Lausanne, CH-1015 Lausanne, Switzerland. Phone: 41 21 692 4111. Fax: 41 21 692 4115. E-mail: walter.wahli@unil.ch.

follicle growth (36, 40). Despite the high expression of PPARβ in follicular keratinocytes throughout the whole process of HF morphogenesis, we provide evidence that PPARβ is important specifically at the developmental stage of hair peg elongation. Most interestingly, we show that the time-dependent activation of PPARβ in HF keratinocytes involves mesenchyme-secreted HGF, which up-regulates the expression of the COX-2 enzyme in keratinocytes, likely leading to the production of PPARβ ligands. We further show that PPARβ protects elongating HFs from apoptosis in vivo, predominantly via the temporal activation of the Akt1 signaling pathway, which plays a key role in the maturation of hair pegs. Such insights into the mesenchyme-epithelium control of PPARβ activation in follicular keratinocytes and antiapoptotic role of Akt1 in HF morphogenesis in vivo are crucial to the molecular understanding of HF growth.

MATERIALS AND METHODS

Reagents. The COX-2 inhibitor (NS-398, no. 349254) and the Akt inhibitor ($C_{30}H_{58}O_{10}$, no. 124005) were from Calbiochem. Recombinant HGF was from Sigma. 5-bromo-4-chloro-3-indolyl phosphate–nitroblue tetrazolium chloride alkaline phosphatase substrates and BrdU were from Roche. All cell culture media and supplies were obtained from Sigma, except the keratinocyte serum-free medium KSFM (Invitrogen). All antibodies were purchased from Santa Cruz Biotechnology, except anti-PPARβ (Affinity Bioreagent), anti-Akt1, anti-phospho-Akt1, anti-glycogen synthase kinase 3β (anti-GSK3β), anti-phospho-GSK3β, anti-Bad, anti-phospho-Bad, anti-FKHR, anti-phospho-FKHR (Cell Signaling), anti-PDK1 (Transduction Laboratories), and anti-β-tubulin (Pharmingen).

Cell culture and transient transfections. Mouse primary keratinocytes were isolated from the epidermis as reported by Hager et al. (14) with the following modifications. The epidermis was separated from the dermis following overnight incubation at 4°C in 2.5 U of dispase/ml. The epidermis was placed in a 50-ml centrifuge tube with 10 ml of culture medium (KSFM), and the tube was given 50 shakes. Keratinocytes were resuspended in KSFM containing 0.05 mM Ca^{2+} and 0.1 ng of epidermal growth factor/ml and were seeded at 10^5 cells per cm^2. Mouse skin organ cultures were performed as followed: 8-mm punch biopsies isolated from the back skin of 1-day-old pups (P1) were transferred to culture inserts (3 μM pore) of a two-chamber tissue culture system (BD Biosciences). Skin explants were cultured at the air-liquid interface in Dulbecco's modified Eagle medium supplemented with 10% normal or delipidated fetal calf serum, 50 μg of vitamin C/ml and 5 μg of gentamicin/ml. After an overnight incubation, explants were treated with the indicated activator or inhibitor or with vehicle for 48 h. Transient transfection assays in keratinocytes were performed using the Superfect reagent (QIAGEN) and luciferase activity (Promega) was measured according to the manufacturers' instruction. The proximal 2-kb mouse COX-2 promoter region was subcloned into the pGL2 luciferase vector (Promega). The mouse PPARβ promoter (41) and peroxisome proliferator response element (PPRE) reporter constructs (10) were described previously.

In situ hybridization, Western blotting, and immunohistochemistry. Digoxigenin-labeled riboprobes were obtained by in vitro transcription, with mouse PPARβ A/B domain cDNA as a template, and in situ hybridization was done as described in Michalik et al. (29). For Western blotting, protein extracts were made in ice-cold lysis buffer (20 mM $Na_2H_2PO_4$, 250 mM NaCl, Triton X-100, 1%, sodium dodecyl sulfate, 0.1%). Equal amounts of protein extracts (20 μg) were resolved by sodium dodecyl sulfate-polyacrylamide gel electrophoresis and electrotransferred onto polyvinylidene difluoride membranes. Membranes were processed as described by the manufacturer (Cell Signaling), and proteins were detected by chemiluminescence (Pierce). To verify the linearity of the chemiluminescent signals obtained, Western blots were also performed using increasing amounts of input proteins (10, 20, and 40 μg). All primary antibodies were used at a dilution of 1:1,000, except for anti-integrin-linked kinase (ILK) and anti-β-tubulin (1:2,500). Immunofluorescent staining (Akt1-S473-P, 1:200; Akt1-T308-P, 1:100; GSK3β-S9-P, 1:50; fluorescein isothiocyanate-conjugated immunoglobulin G secondary antibody, 1:200) was performed as described by the manufacturer (Cell Signaling). Colorimetric immunostaining (PPARβ, 1:200; COX-2, 1:25) was carried out using the ABC-peroxidase method (Vector Laboratories) and revealed using diaminobenzidine with (PPARβ) or without (COX-2) metal enhancer (Sigma).

Proliferation and apoptotic assays. The number of proliferative and apoptotic keratinocytes in the $PPAR\beta^{+/+}$ and $PPAR\beta^{-/-}$ epidermis and HFs was analyzed on longitudinal cryosections through the developing skin (35). To detect the proliferative cell nuclear antigen (PCNA) proliferative marker, tissue sections were incubated at 95°C in 0.01 M citric acid (pH 6.0) for 20 min, followed by a 30-min cooldown. Sections were treated with 5% bovine serum albumin in phosphate-buffered saline for 1 h at room temperature to reduce nonspecific staining and then with primary antibodies (1:50) overnight at 4°C. For BrdU labeling, mice were injected subcutaneously with BrdU (50 μg per gram of body weight) and sacrificed 2 h later. Skin samples were incubated for 90 min with an anti-BrdU monoclonal antibody conjugated with peroxidase (Roche). Colorimetric immunostaining was revealed using diaminobenzidine with (PCNA) or without (BrdU) metal enhancer. The sections were counterstained with hematoxylin-eosin. The apoptotic keratinocytes were detected using the terminal deoxynucleotidyltransferase-mediated dUTP-biotin nick end labeling (TUNEL) assay according to the manufacturer's protocol (Roche). Briefly, cryosections were fixed in 4% formaldehyde for 20 min at room temperature, washed, and then permeabilized (Triton X-100, 0.1%, sodium citrate, 0.1%) for 2 min on ice. The fragmented DNA was labeled using fluorescent nucleotides, and slides were subsequently counterstained with DAPI (4′,6′-diamidino-2-phenylindole) for microscopic observation.

Quantitative histomorphometry. The percentage of HFs in different stages of morphogenesis was assessed according to accepted morphological and histological criteria by using longitudinal cryosections (35). To precisely identify the substages of HF development, histochemical detection of endogenous alkaline phosphatase activity, as a sensitive marker of the developing dermal papilla, was performed using 5-bromo-4-chloro-3-indolyl phosphate–nitroblue tetrazolium chloride substrates (35). The percentage of HFs in defined stages of morphogenesis was evaluated, and hair morphogenesis mean stages (hair scores) were calculated accordingly. At least 600 to 800 HFs from four different $PPAR\beta^{+/+}$ or $PPAR\beta^{-/-}$ mice or 500 to 600 HFs from three different $Akt1^{+/-}$ or $Akt1^{-/-}$ mice of defined age were analyzed. For analysis on organ culture, four skin biopsies of each experimental group were investigated. Skin thickness was assessed on hematoxylin–eosin-stained cryosections by using the ImageJ free software. The independent Student's *t* test for unpaired samples was used for all statistical analyses.

RESULTS

PPARβ is highly expressed in the keratinocytes of developing hair follicles. The persistence of PPARβ expression at the mRNA level in postnatal HFs while it was disappearing from the interfollicular epidermis (29) suggested that PPARβ might play an important role in HF morphogenesis. Therefore, we first performed a detailed analysis of the expression of PPARβ in the developing skin of mice from embryonic day (E)16.5 to postnatal day (P)10, by in situ hybridization (Fig. 1A) and immunohistochemistry (Fig. 1B), with the skin of mutant $PPAR\beta^{-/-}$ mice as a negative control (Fig. 1B). The PPARβ protein was found to be abundant in the basal layer of the embryonic interfollicular epidermis and in follicular keratinocytes, with lower expression in the dermal fibroblasts. Furthermore, PPARβ was mainly detected in the nuclear compartment (Fig. 1). During HF induction (E14.5 to E16.5), PPARβ was expressed in follicular epithelial precursors, which appear first as placodes in the otherwise uniform surface epithelium. During subsequent downgrowth of the nascent HFs into the dermis (Fig. 1) (P1), PPARβ became highly expressed in hair germs (developmental stage 2; see Fig. 10) and elongated hair pegs (stages 3 to 4). By P4, PPARβ mRNA and protein expression decreased in the interfollicular epidermis, consistent with previous observations (29), and became mainly restricted to the outer root sheath (ORS) and hair matrix cells (Fig. 1) (P10). However, PPARβ was absent in the developing and mature dermal papilla (Fig. 1) (P1 to P10).

Altogether, the high expression of PPARβ in defined epi-

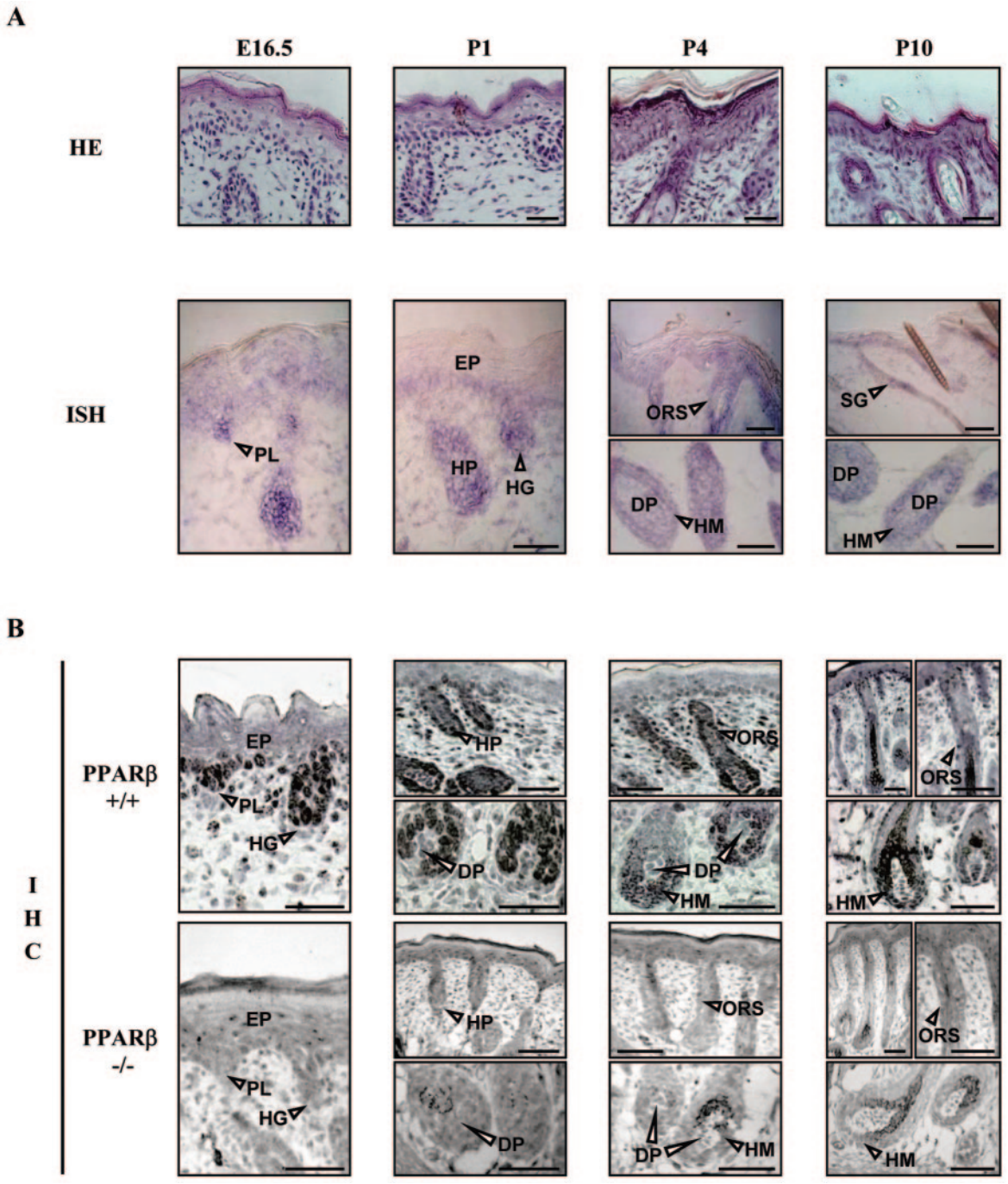

FIG. 1. Expression of PPARβ in the developing hair follicle. (A) Cryosections of mouse PPARβ$^{+/+}$ dorsal skin from E16.5 and from P1 to P10 were stained with hematoxylin-eosin (HE) or were processed for the detection of PPARβ by in situ hybridization (ISH). (B) The detection of PPARβ at the protein level was performed in PPARβ$^{+/+}$ and PPARβ$^{-/-}$ skin by immunohistochemistry (IHC). PPARβ is expressed in the interfollicular epidermis (EP) and hair placodes (PL) of stage 1 HFs, in elongating hair germs (HG) and hair pegs (HP) of early HFs (stages 2 to 4), and in the ORS, hair matrix (HM), and sebaceous gland (SG) cells of mature PPARβ$^{+/+}$ HFs. No staining was observed in the dermal papilla fibroblasts (DP). Magnification bars, 50 μm.

thelial follicular compartments throughout HF morphogenesis suggests a so-far-unidentified function of PPARβ in the control of HF maturation that is characterized by expansive tissue growth.

PPARβ regulates postnatal hair follicle morphogenesis. To explore the functional role of PPARβ during HF morphogenesis, we studied the dynamic of HF development in the back skin of age-matched wild-type (WT) PPARβ$^{+/+}$ and PPARβ$^{-/-}$ mice (K. Nadra et al., submitted for publication) (29) by quantitative histomorphometry. As shown in Fig. 2A (top panel), HFs from E16 to P1 were similarly developed in PPARβ$^{-/-}$ mice and WT controls, indicating that PPARβ is

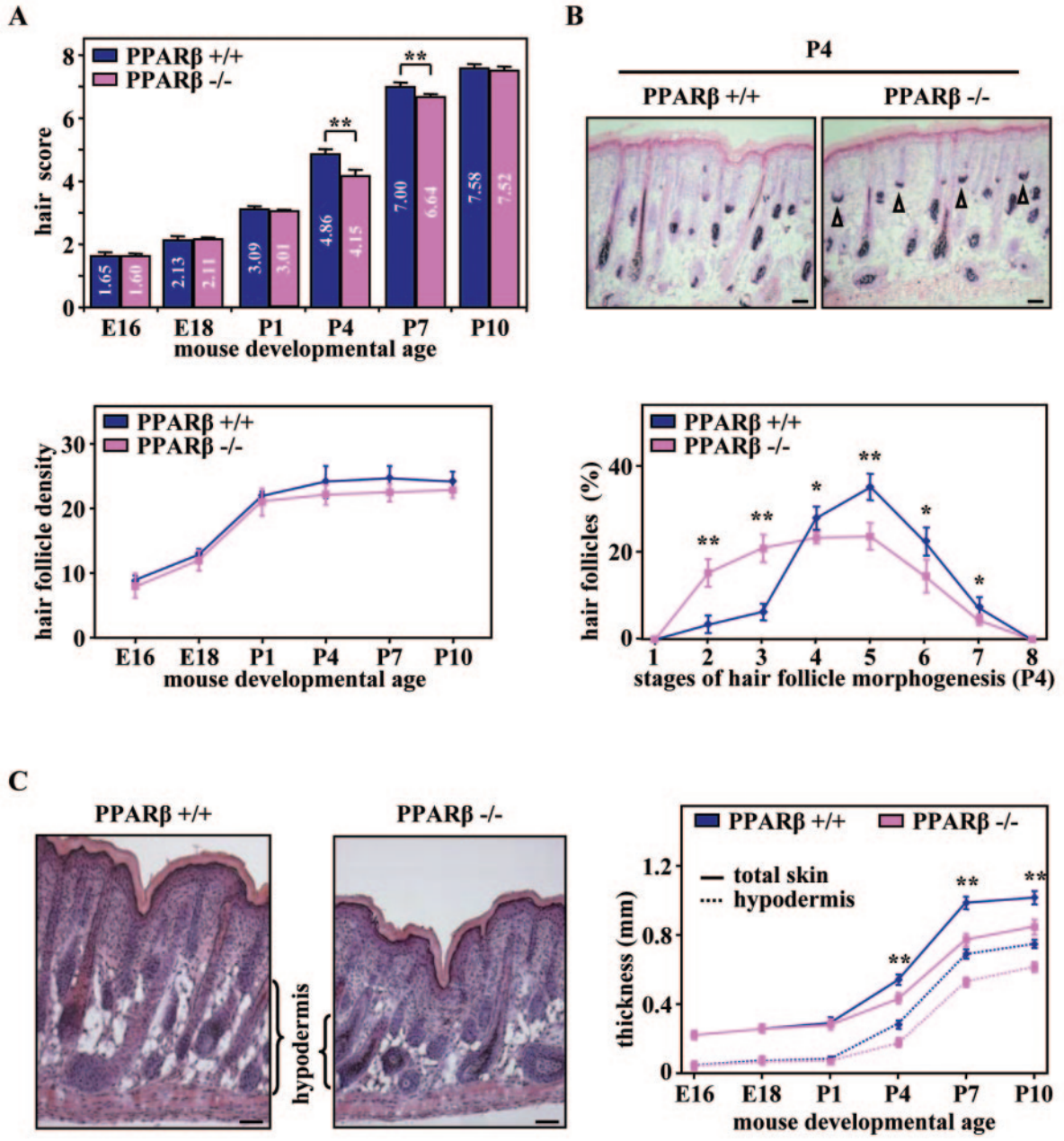

FIG. 2. Retardation of postnatal hair follicle development in PPARβ-null mice. (A) The hair score (top panel) and the total number of HFs per millimeter of epidermis length (hair follicle density; bottom panel) were evaluated by quantitative histomorphometry in PPARβ wild-type ($PPAR\beta^{+/+}$) and PPARβ knockout ($PPAR\beta^{-/-}$) mice at the indicated embryonic or postnatal developmental age. (B) Representative staining of endogenous alkaline phosphatase activity in dermal papilla cells (top panel) and detailed analysis of the percentage of HFs at distinct stages of morphogenesis (bottom panel) in $PPAR\beta^{+/+}$ and $PPAR\beta^{-/-}$ skin at day P4 are given. Arrowheads indicate the persistence of early HFs in the $PPAR\beta^{-/-}$ skin. (C) Skin sections from four different $PPAR\beta^{+/+}$ and $PPAR\beta^{-/-}$ mice at P4 were stained with hematoxylin-eosin (left panels). The thickness of total skin and hypodermis were determined at the indicated mouse developmental age by quantitative histomorphometry (right panel). The independent Student's *t* test was used to assess the statistical significance of phenotype differences between the PPARβ genotypes ($PPAR\beta^{+/+}$ versus $PPAR\beta^{-/-}$) (*, $P < 0.05$; **, $P < 0.01$). Magnification bars, 50 μm.

dispensable for the initiation of HF development. Interestingly, follicular growth was significantly delayed in $PPAR\beta^{-/-}$ mice by P4, as reflected by the lower hair score (Fig. 2A, top panel). Indeed, PPARβ-mutant skin displayed a reduced number of HFs at the advanced stages of morphogenesis (HF developmental stages 4 to 7; see Fig. 10), with a corresponding increase in the number of early hair germs and hair pegs (stages 2 to 3) that are characterized by the presence of mesenchyme at their base (Fig. 2B). Furthermore, as another important indicator of retarded HF development in $PPAR\beta^{-/-}$ mice, a significant decrease in the thickness of skin hypodermis was observed from P4 onwards, reflected by a reduced overall

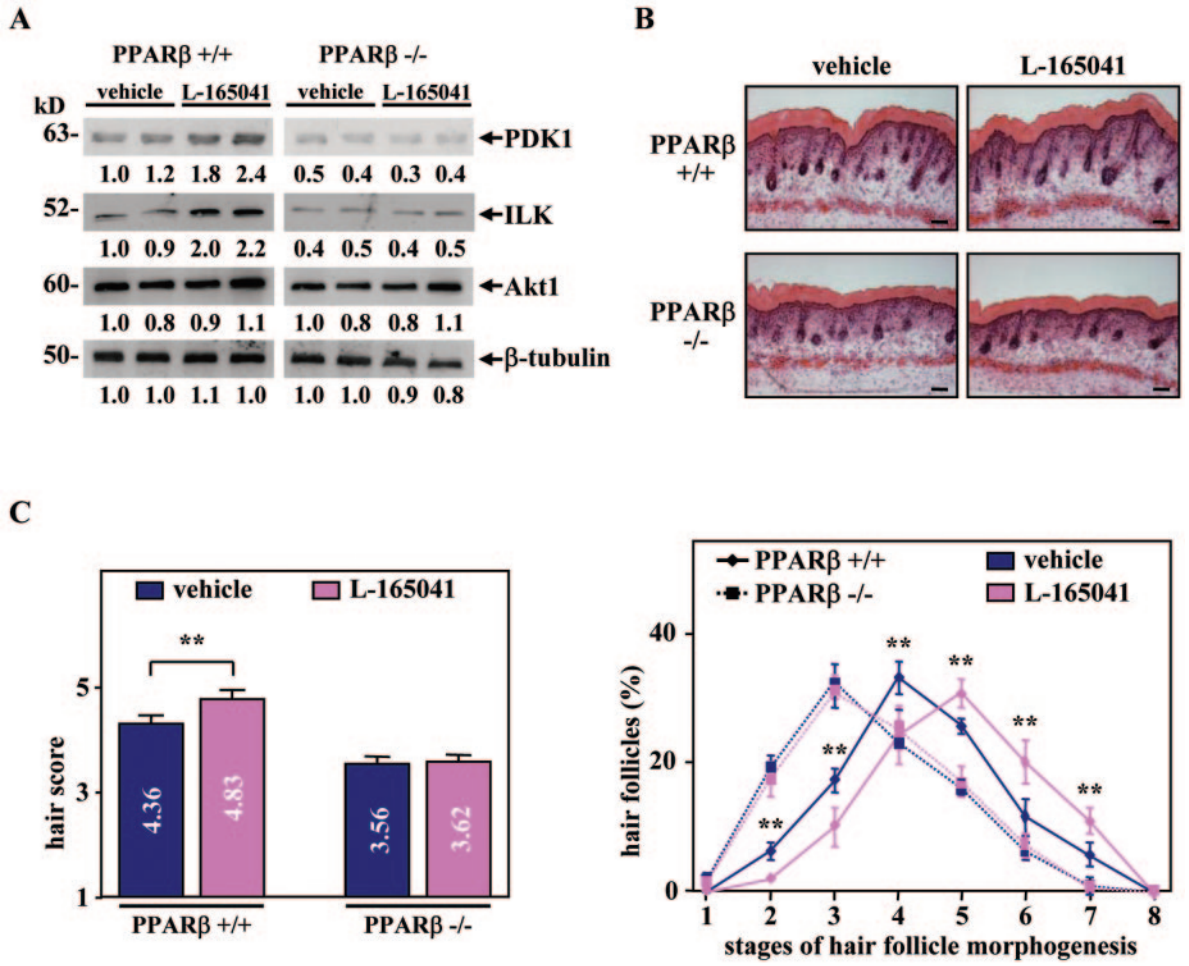

FIG. 3. Activation of PPARβ accelerates hair follicle development in skin organ culture. (A) Total cellular proteins from PPARβ$^{+/+}$ and PPARβ$^{-/-}$ skin explants treated (L-165041) every 24 h for 2 days with 5 μM of PPARβ ligand L-165041 or not treated (dimethyl sulfoxide; vehicle) were used for Western blot analysis. Changes, indicated below each band, represent the mean of two independent experiments. β-Tubulin was used as internal control. The apparent molecular mass is indicated for each protein. (B) Longitudinal cryosections from four different PPARβ$^{+/+}$ and PPARβ$^{-/-}$ skin explants treated (L-165041) or not treated (vehicle) were stained for endogenous alkaline phosphatase activity as a marker for the developing dermal papilla and counterstained with hematoxylin-eosin. Magnification bars, 50 μm. (C) The hair scores (left panel) and the percentage of HFs at distinct stages of morphogenesis (right panel) were determined by quantitative histomorphometry in PPARβ$^{+/+}$ and PPARβ$^{-/-}$ skin explants treated or with L-165041 or not treated. Independent Student's *t* test: *, $P < 0.05$; **, $P < 0.01$.

skin thickness (Fig. 2C). However, no significant difference in the total number of HFs was found between PPARβ$^{-/-}$ and WT skin (Fig. 2A, bottom panel), which is consistent with the absence of defects during HF induction. Interestingly, HF development was still delayed at P7 in PPARβ$^{-/-}$ skin, but the first hair coat of the mice appeared indistinguishable from that of WT mice at P10, presumably because other mechanisms regulating HF formation compensate for the lack of PPARβ (Fig. 2A).

To further demonstrate the biological significance of these observations, we next assessed the effect of the synthetic PPARβ ligand L-165041 on HF development in PPARβ$^{+/+}$ and PPARβ$^{-/-}$ skin organ culture. As shown in Fig. 3A, PPARβ$^{+/+}$ explants treated with the PPARβ agonist showed an increase in the expression of the two PPARβ target genes, 3-phosphoinositide-dependent kinase 1 (PDK1) and ILK (11). Interestingly, treatment of PPARβ$^{+/+}$ skin with L-165041 significantly accelerates HF development, as reflected by the higher hair morphogenesis score (Fig. 3B and C). In addition, the stimulatory effect of L-165041 on HF growth is PPARβ dependent, as it was not observed in the PPARβ$^{-/-}$ explants (Fig. 3C).

Together, these results demonstrate that PPARβ does not significantly affect embryonic development of mouse skin but regulates postnatal HF growth shortly after its induction, by controlling hair peg maturation into the dermis.

Increased apoptosis in early hair follicles of PPARβ-deficient skin. HF morphogenesis depends on a delicate balance between cell proliferation and apoptosis (27). To elucidate the function of PPARβ in the control of hair growth, apoptosis and proliferation indexes were assessed during HF morphogenesis by using TUNEL, as well as immunodetection of the PCNA and bromodeoxyuridine (BrdU).

As shown in Fig. 4A, proliferative PCNA and BrdU staining were homogeneously distributed in early hair germs and hair pegs (P1) and became restricted to ORS and hair matrix cells

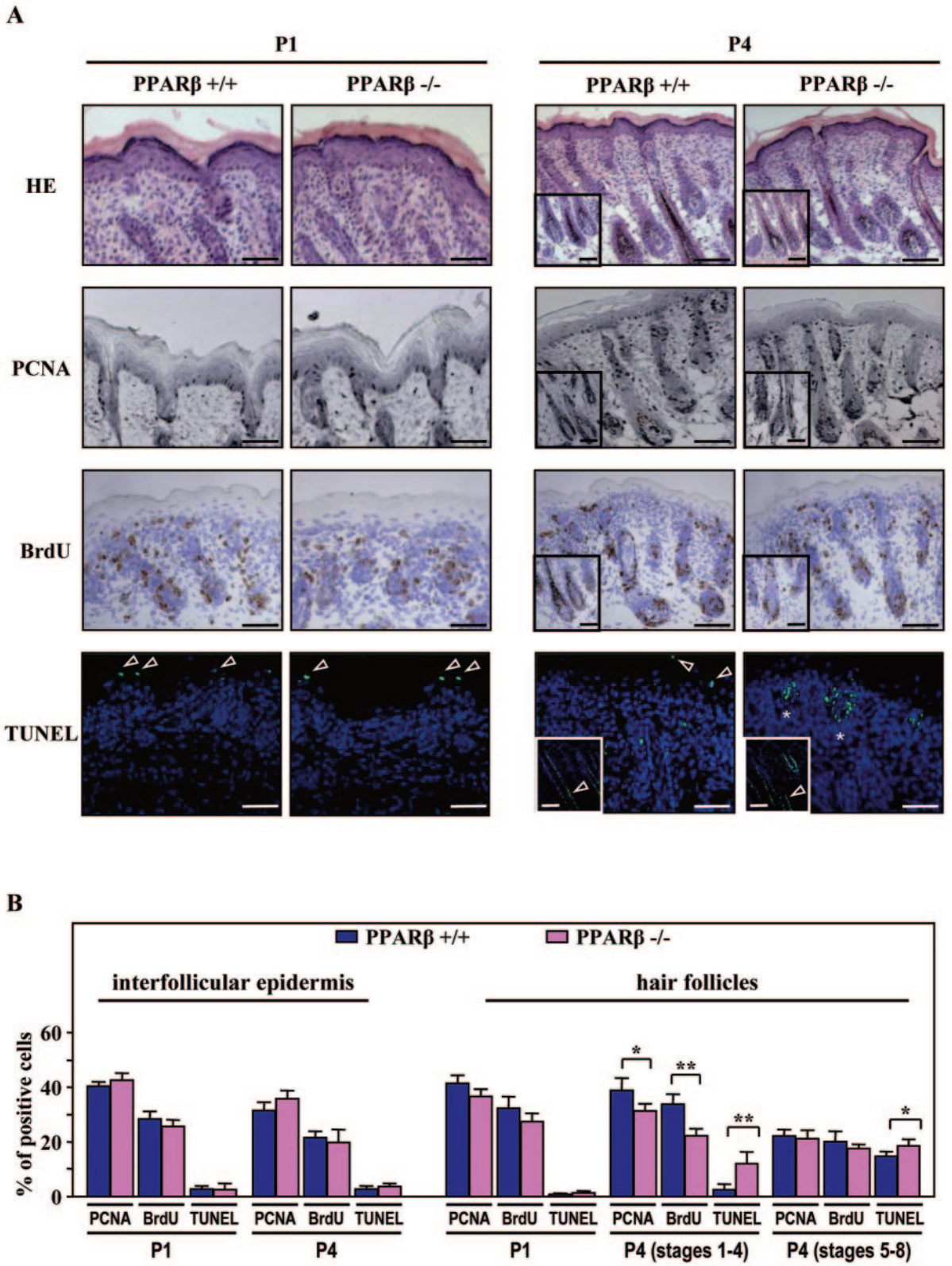

FIG. 4. PPARβ protects keratinocytes against apoptosis during hair follicle development. (A) Cryosections of developing PPARβ$^{+/+}$ and PPARβ$^{-/-}$ skin were stained for PCNA and BrdU (proliferation markers) or TUNEL (apoptotic marker). The figure shows representative fields of the labeling obtained at day P1 and P4. In PPARβ$^{+/+}$ skin, suprabasal layers of the interfollicular epidermis and advanced HFs (stages 5 to 8; inserts) show TUNEL-positive staining (arrowheads). Apoptotic cells were already detected in early HFs of PPARβ$^{-/-}$ skin at P4 (stages 3 to 4; asterisks). Cell nuclei were counterstained with DAPI. Magnification bars, 50 μm. HE, hematoxylin-eosin. (B) The percentages of PCNA-, BrdU-, and TUNEL-positive cells were evaluated among the population of PPARβ$^{+/+}$ and PPARβ$^{-/-}$ interfollicular (interfollicular epidermis) or follicular (hair follicles) keratinocytes at P1 and P4. Due to irregular patterns of proliferation and apoptosis during HF morphogenesis, developmental stages were separated into early (stages 1 to 4) and advanced (stages 5 to 8) HFs at P4. Independent Student's *t* test: ∗, $P < 0.05$; ∗∗, $P < 0.01$.

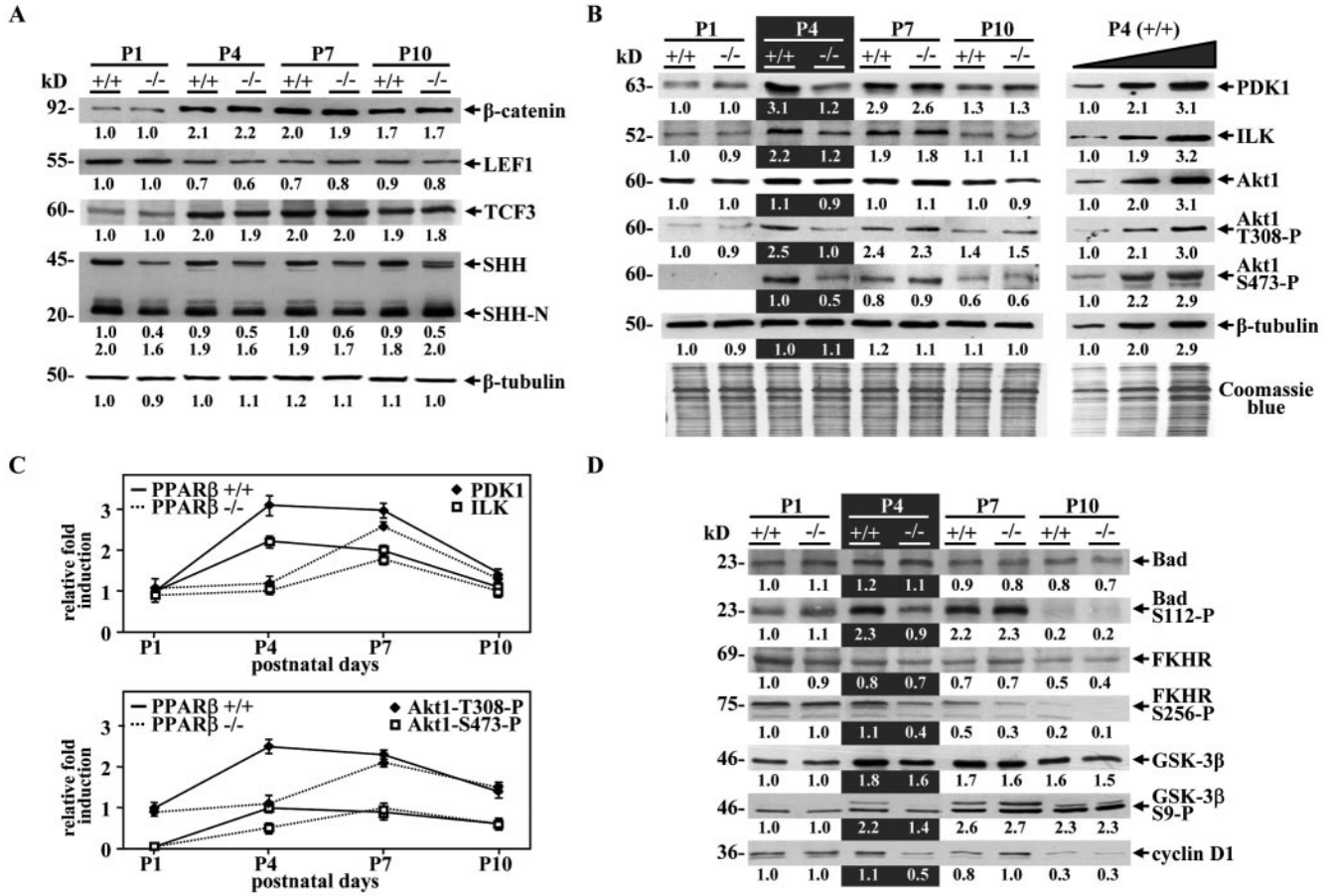

FIG. 5. PPARβ modulates the Akt1 signaling pathway in mouse postnatal skin. (A) Western blot assays were carried out using equal amounts (20 μg) of proteins from PPARβ$^{+/+}$ (+/+) and PPARβ$^{-/-}$ (−/−) mouse skin tissues at the indicated postnatal days (P1 to P10). A representative experiment is shown. Changes, indicated below each band, represent the mean of three independent experiments, after normalization to the PPARβ$^{+/+}$ at P1. β-Tubulin was used as internal control. The apparent molecular mass is indicated for each protein. (B) The expression of various actors of the Akt1 pathway was assessed by Western blots as described in panel A, and equal protein loading was confirmed using Coomassie blue staining of blots (Coomassie blue). To verify the linearity of the signals, Western blots were also performed using increasing amounts of input proteins (10, 20, and 40 μg) from PPARβ$^{+/+}$ mouse skin at P4 (P4, +/+; right panel). (C) Quantification of relative PDK1/ILK and phosphorylated Akt1 protein expression in postnatal skin from P1 to P10 in PPARβ$^{+/+}$ and PPARβ$^{-/-}$ mice. (D) Western blot assays were performed as in panel A by using the indicated antibodies.

of HFs by P4. Quantitative analysis of PCNA- and BrdU-positive cells revealed a slight decrease (10 to 20%) in the number of proliferative keratinocytes between PPARβ-null and WT pups in early HFs at P4 (stages 1 to 4), with no significant difference in the interfollicular epidermis (Fig. 4B). Throughout HF morphogenesis, TUNEL-positive cells were absent during the first stages of HF development (stages 1 to 4) and appeared only in the inner root sheath and ORS of mature PPARβ$^{+/+}$ HFs (Fig. 4A) (P4). In contrast, increased apoptosis was seen in developing HFs of PPARβ$^{-/-}$ skin at P4, with the appearance of TUNEL-positive keratinocytes in early HFs (Fig. 4A and B) (stages 1 to 4). No significant difference was observed in the proportion of apoptotic cells restricted to upper suprabasal layers of the interfollicular epidermis (Fig. 4B).

Consistent with the antiapoptotic role of PPARβ previously reported in cell culture (11), the balance between proliferation and apoptosis is altered during the development of PPARβ$^{-/-}$ HFs in vivo. Indeed, the rate of apoptosis associated with early postnatal HF development is enhanced in the absence of PPARβ and may explain, at least in part, the delayed HF morphogenesis observed in PPARβ-null mice.

β-Catenin/TCF and Sonic hedgehog expression is not affected in PPARβ-null skin. To further explore the molecular mechanisms by which PPARβ acts in regulating HF growth, we studied the expression of β-catenin/TCF and SHH signaling molecules that are essential for HF induction and early development (31).

From P1 to P10, no difference between PPARβ$^{+/+}$ and PPARβ$^{-/-}$ mouse skin was observed in the expression levels of β-catenin and of two members of the TCF family present in HFs, LEF1 and TCF3 (Fig. 5A). We next assessed the expression of SHH, an important actor in both the formation of dermal papilla and the proliferation of hair pegs following HF induction, a developmental phase which coincides with delayed HF development in PPARβ-null skin (Fig. 2). No significant difference in biologically active SHH (SHH-N) protein expression through postnatal skin development was observed between PPARβ$^{+/+}$ and PPARβ $^{-/-}$ mice, whereas inactive full-

length protein (SHH) was decreased by ~2-fold in the PPARβ-deficient skin (Fig. 5A).

These findings are consistent with the absence of defect at the time of HF induction in PPARβ-null skin and suggest that β-catenin/TCF and SHH are not the underlying cause of premature apoptosis observed in PPARβ-null follicular keratinocytes.

Activation of the Akt1 signaling pathway by PPARβ is necessary for the development of hair follicles. We previously reported that PPARβ- and Akt1-null mice share many similar phenotypes, suggesting a broad action of PPARβ via Akt1 on several biological processes, in addition to skin wound healing (10). Interestingly, impaired skin development with defects in HF growth has recently been reported in Akt1/Akt2 double-knockout (DKO) animals (36). Thus, we examined the expression of various actors of the Akt1 pathway during postnatal HF development, by using quantitative Western blot assays (Fig. 5B). In WT skin, Western blot analysis revealed an up-regulation from P1 to P4 of the two PPARβ target genes PDK1 and ILK, and as a consequence, an increased phosphorylation of Akt1 at T308 (Akt1-T308-P) and S473 (Akt1-S473-P), respectively (Fig. 5B). High expression of these proteins persisted throughout P7 but declined when HF morphogenesis was completed (P10). Interestingly, the expression profiles of PDK1, ILK, and phosphorylated Akt1 were delayed and peaked at P7 in the PPARβ$^{-/-}$ mice compared to the WT controls (Fig. 5C), probably due to the activity of other regulators of ILK and/or PDK1 expression which remain to be identified. The reduced Akt1 activity in PPARβ-null skin at P4 was reflected by lower phosphorylated Bad (Bad-S112-P), forkhead in rhabdomyosarcoma (FKHR-S256-P), and glycogen synthase kinase-3β (GSK-3β-S9-P) levels, without changes in their total protein expression levels (Fig. 5D). Bad/FKHR and GSK-3β are major direct targets of Akt1 and are involved in its anti-apoptotic and proliferative activities, respectively (6). Furthermore, a decrease in the expression of cyclin D1, whose turnover is regulated by GSK-3β, was observed at P4 in PPARβ$^{-/-}$ compared to PPARβ$^{+/+}$ skin (Fig. 5D), and this may explain the slight decrease in proliferation observed in early PPARβ$^{-/-}$ HFs (Fig. 4B).

Immunofluorescence analysis of phosphorylated active Akt1 distribution showed a predominant expression of Akt1-T308-P and Akt1-S473-P in both follicular and interfollicular keratinocytes of the developing skin (Fig. 6A). Similar to PPARβ expression in the developing HF (Fig. 1), phosphorylated Akt1 was high in elongating hair germs and hair pegs (Fig. 6A) (P4) and became confined to ORS keratinocytes of the mature HFs (P7 to P10). However, active Akt1 was below detection levels in dermal papilla cells (Fig. 6A) (P4 to P10). Interestingly, whereas the expression of Akt1-S473-P was only confined to basal interfollicular keratinocytes, Akt1-T308-P was also detected in the first suprabasal layers of the interfollicular epidermis (Fig. 6A), possibly forming a gradient of Akt1 activity in the epidermis. Similar immunofluorescence assays performed in PPARβ$^{-/-}$ skin revealed a reduced staining of both Akt1-T308-P and Akt1-S473-P at P4 in many keratinocytes of HFs (Fig. 6B). Consistent with Akt1-mediated phosphorylation of GSK-3β, the expression of GSK-3β-S9-P overlapped with that of phosphorylated Akt1 in elongating hair pegs, with a parallel decreased staining in PPARβ$^{-/-}$ skin at P4 (Fig. 6B). In addition, GSK-3β-S9-P was also observed in hair shaft precursors of differentiating HFs (Fig. 6B), where the Wnt pathway has been shown to be activated (31).

Altogether, these results indicate that PPARβ, phosphorylated Akt1, and phosphorylated GSK-3β strictly colocalize in the epithelial compartment of early HFs and that the delayed activation of Akt1 at P4 in PPARβ$^{-/-}$ skin correlates with increased apoptosis and slightly reduced proliferation observed in vivo in developing HFs.

Akt1 activity is required for hair peg elongation during hair follicle development. Since PPARβ exerts its antiapoptotic effects via the Akt1 signaling pathway in primary keratinocytes (11), we next compared the dynamic of HF development in Akt1$^{-/-}$ and Akt1 heterozygous (Akt1$^{+/-}$) control skin (45), to ensure the same genetic background, at days P1 and P4. Similar to HF development in PPARβ-null mice (Fig. 2), follicular growth was significantly delayed in Akt1$^{-/-}$ skin at P4 (Fig. 7A), as reflected by the reduced hair score (Akt1$^{-/-}$ versus Akt1$^{+/-}$: 3.82 ± 0.10 versus 4.70 ± 0.19) (Fig. 7B, left panel). Indeed, Akt1-null skin displayed an increased proportion of underdeveloped HFs (Fig. 7B, right panel) that was associated with a dramatic decrease in hypodermis thickness (Fig. 7C), when compared to the Akt1$^{+/-}$ control.

To further demonstrate the role of the Akt1 pathway in HF growth, we next assessed the effect of a specific Akt inhibitor ($C_{30}H_{58}O_{10}$) in skin organ culture. To mimic the absence of Akt1 activation at P4 observed in PPARβ$^{-/-}$ animals (Fig. 5C), skin explants were taken after HF induction from the back skin of P1 mice and were cultured until P4 in the absence or presence of the inhibitor. As shown in Fig. 8A, explants treated with the Akt inhibitor showed a significant decrease in phosphorylated Akt1 protein levels, which was translated into reduced GSK-3β phosphorylation and cyclin D1 expression. Furthermore, and as recently observed with other Akt inhibitors, S473 phosphorylation was inhibited to a greater extent than T308, probably due to a better recovery of the T308 phosphorylation site (7). Interestingly, inhibition of Akt activity in PPARβ$^{+/+}$ explants strongly delayed HF morphogenesis, as reflected by the reduced hair score (Fig. 8B, left panel). The effect of the Akt inhibitor was weaker in PPARβ$^{-/-}$ explants (Fig. 8B), because PPARβ-deficient skin already exhibits low active Akt1. Indeed, similar to the PPARβ-null skin, explants treated with the Akt inhibitor displayed a higher proportion of underdeveloped HFs (stages 2 to 3) (Fig. 8B, right panel). Importantly, a 1.4- to 1.6-fold decrease and a strong 6- to 7-fold increase in the percentage of proliferating and apoptotic keratinocytes, respectively, were observed in early HFs of Akt inhibitor-treated PPARβ$^{+/+}$ explants (Fig. 8C).

These results demonstrate that the temporal control of the activity of Akt1 is crucial for normal development of early HFs. Thus, an absence of PPARβ-mediated activation of the anti-apoptotic Akt1 signaling pathway in the PPARβ-null follicular keratinocytes provides an explanation for the delayed HF morphogenesis.

COX-2-dependent activation of PPARβ in elongating hair pegs. We revealed here that despite the high expression of PPARβ in the early epithelial precursors at the time of HF induction, its role becomes important specifically at later stage of hair peg maturation. This suggests that the timely ligand-dependent activation of PPARβ in developing hair pegs may

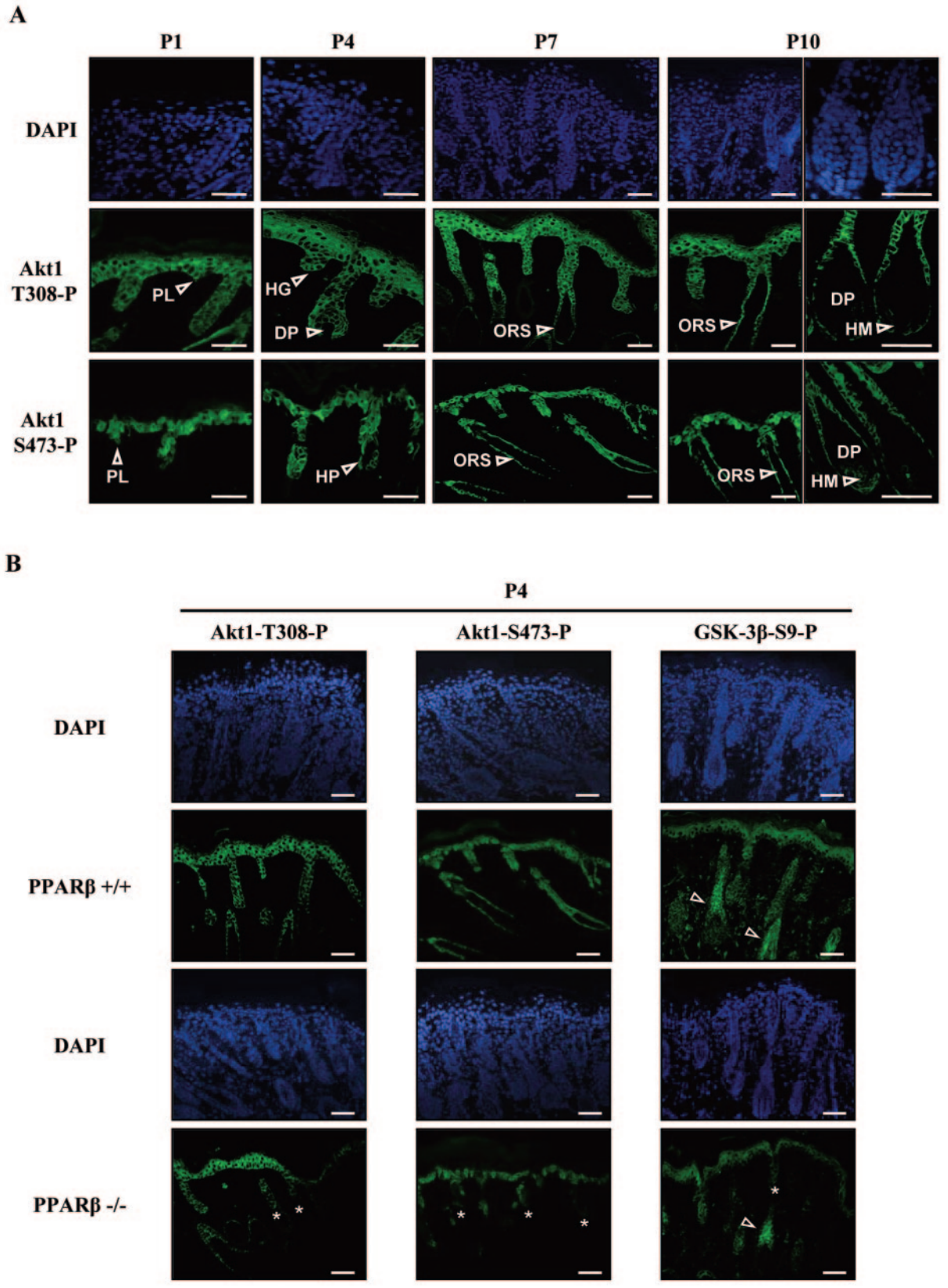

FIG. 6. Phosphorylated Akt1 is expressed in the epithelial compartment of developing hair follicles. (A) The spatiotemporal expression pattern of phosphorylated Akt1 at both T308 (Akt1-T308-P) and S473 (Akt1-S473-P) in the developing postnatal mouse skin (P1 to P10) was assessed by immunofluorescence. Phosphorylated Akt1 colocalizes with PPARβ in hair placodes (PL), hair germs (HG), and hair pegs (HP) of developing HFs at early stages (P1 to P4), and then became restricted to ORS keratinocytes of mature HFs (ORS; P7to P10), with no detectable expression in hair

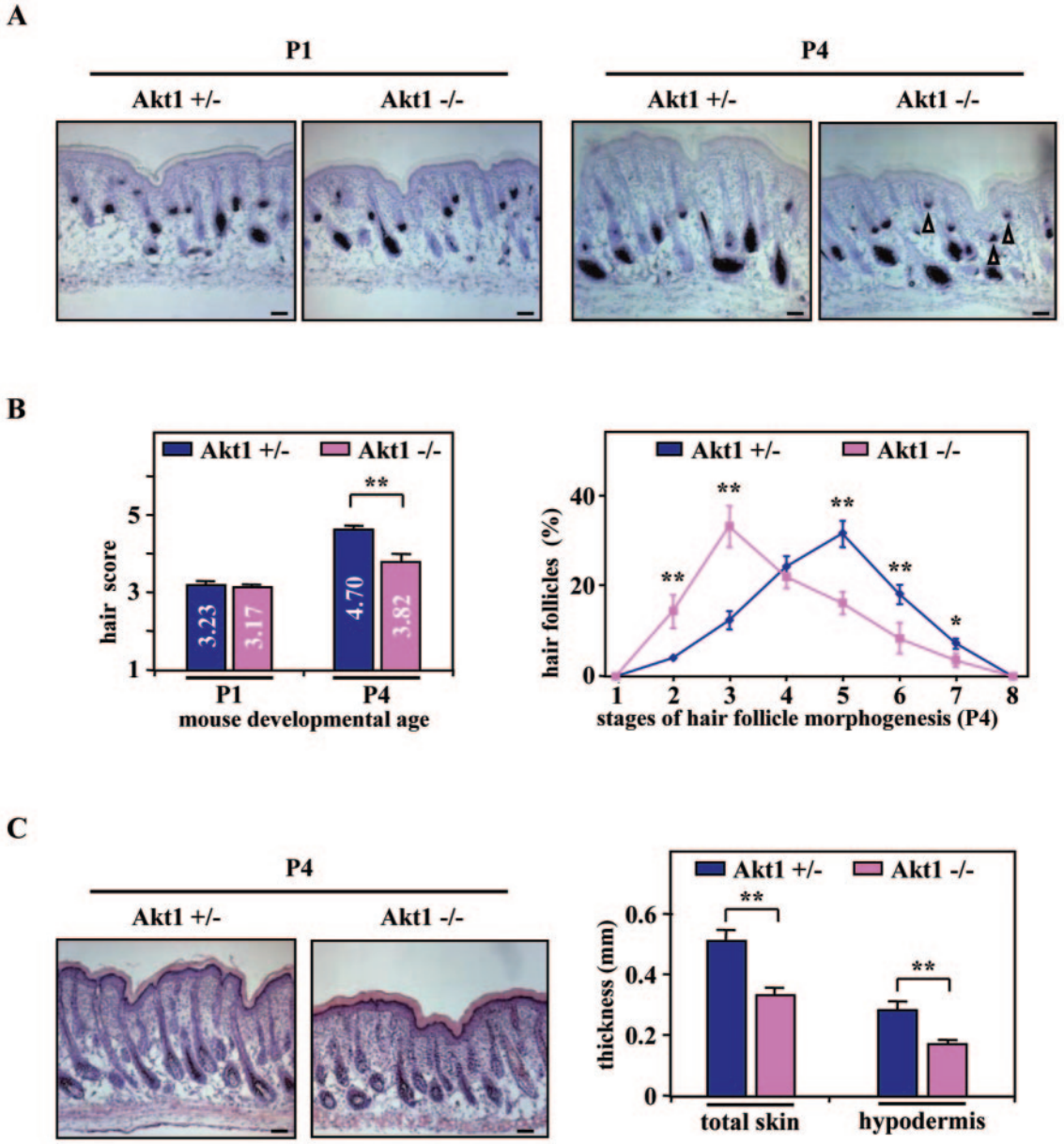

FIG. 7. Retardation of hair follicle development in Akt1-knockout mice. (A) Representative staining of endogenous alkaline phosphatase in Akt1 heterozygous ($Akt1^{+/-}$) and Akt1-knockout ($Akt1^{-/-}$) skin at P1 (left panels) and P4 (right panels) are given. Arrowheads indicate the persistence of early HFs in the $Akt1^{-/-}$ skin. (B) The hair scores (left panel) and detailed analysis of the percentage of HFs at distinct stages of morphogenesis (right panel) in three different $Akt1^{+/-}$ and $Akt1^{-/-}$ skin were assessed by quantitative histomorphometry at the indicated developmental age. (C) Skin sections of $Akt1^{+/-}$ and $Akt1^{-/-}$ mice at P4 were stained with hematoxylin-eosin (left panels), and the thickness of total skin and hypodermis were determined by histomorphometry (right panel). Independent Student's t test: *, $P < 0.05$; **, $P < 0.01$. Magnification bars, 50 μm.

be coordinated with the temporal activation of an associated cascade, which may be triggered by the second dermal signal (31).

The COX-2 enzyme, whose prostaglandin products were described as potent PPARβ ligands (24, 43), has recently been shown to be expressed and active in the developing HF (33). Consistent with the latter report, the expression of COX-2 was high in hair germs and hair pegs of early HF stages, as well as

matrix (HM; P10) and dermal papilla cells (DP; P10). (B) Skin sections of $PPAR\beta^{+/+}$ and $PPAR\beta^{-/-}$ mice were compared at P4 for the presence of phosphorylated Akt1 and phosphorylated GSK-3β at S9 (GSK-3β-S9). Reduced immunostaining of phosphorylation sites of both Akt1 and GSK-3β was observed in follicular keratinocytes of $PPAR\beta^{-/-}$ skin (asterisks). Arrowheads indicate the expression of GSK-3β-S9 in the hair shaft precursors (precortex region) of differentiating HFs. Cell nuclei were counterstained with DAPI. Magnification bars, 50 μm.

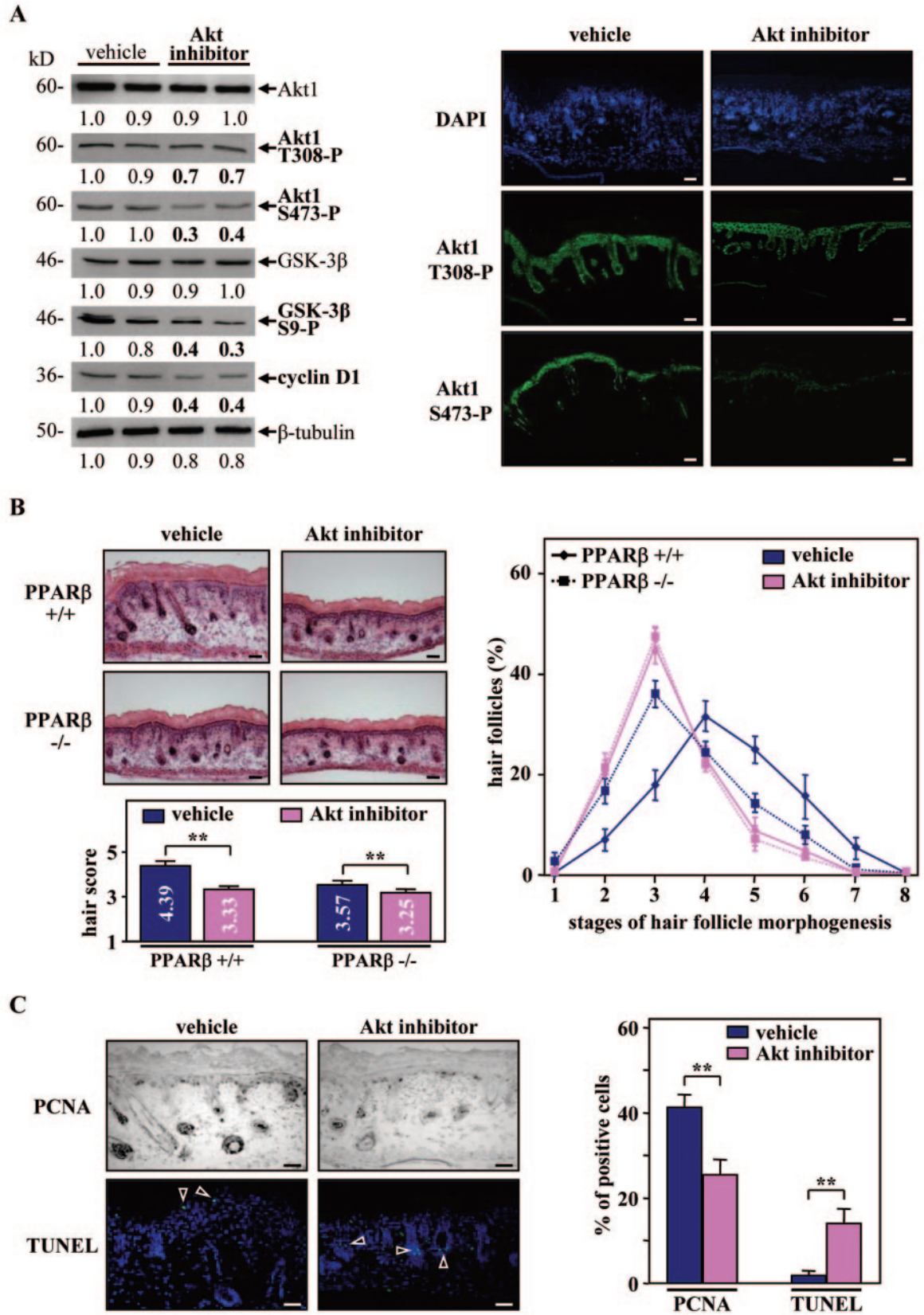

FIG. 8. Inhibition of Akt1 activity blocks hair follicle development in organ culture. (A) Total cellular proteins from PPARβ$^{+/+}$ explants treated (Akt inhibitor) for 48 h with the Akt inhibitor or not treated (dimethyl sulfoxide; vehicle) were used for Western blot analysis (left panel). Explants treated with the Akt inhibitor showed a decrease in the phosphorylation state of Akt1 at both T308 and S473. Decreased Akt1 activity is reflected by reduced phosphorylation of GSK-3β at S9 and reduced cyclin D1 expression. A similar reduction in the expression of phosphorylated

in sebaceous gland cells of mature HFs (Fig. 9A, top panels). Most interestingly, the expression of COX-2 was up-regulated during skin development from P1 to P4 (Fig. 9A, bottom panel), recapitulating the PPARβ-mediated Akt1 activation profile (Fig. 5C). To further assess a possible contribution of COX-2 to HF development, we examined the effect of COX-2 inhibition on skin organ culture. Treatment of WT postnatal skin explants with the specific COX-2 inhibitor NS-398 significantly delayed early HF morphogenesis in a dose-dependent manner and at similar stages as in PPARβ-null skin (Fig. 9B and C). These results were reminiscent of the delayed HF morphogenesis observed in PPARβ- and Akt1-null skin. They are consistent with a model in which COX-2 modulates PPARβ activity in the developing HF, possibly by the production of specific PPARβ ligands.

Paracrine effect of HGF on COX-2 expression and PPARβ activity in keratinocytes. COX-2 expression is stimulated by a wide variety of cytokines and growth factors, including HGF in cancer cells (46). Most interestingly, this paracrine factor has been identified as a second dermal signal that leads to HF elongation (31). Indeed, HGF is expressed specifically in dermal papilla fibroblasts, whereas its receptor, Met, is expressed in the follicular epithelium. Moreover, HGF expression peaks during the initial phases of HF growth and was shown to accelerate HF morphogenesis at P3 (26).

To study the effect of HGF on COX-2 and PPARβ expression in keratinocytes, transient transfections were done using the proximal mouse promoter of both *COX-2* and *PPAR*β genes. As shown in Fig. 9D, HGF increased the activity of the COX-2 promoter in a dose-dependent manner but did not affect PPARβ promoter activity. In agreement with this result, treatment of PPARβ$^{+/+}$ and PPARβ$^{-/-}$ primary keratinocytes with HGF induced COX-2 protein expression (Fig. 9D). In parallel, we showed that HGF increased the protein levels of ILK, PDK1, and phosphorylated Akt1 in PPARβ$^{+/+}$ cells (Fig. 9E). Importantly, the effect of HGF was strongly diminished in both PPARβ$^{-/-}$ cells and PPARβ$^{+/+}$ cells pretreated with the COX-2 inhibitor, suggesting that the HGF-mediated activation of the Akt1 pathway is dependent on both PPARβ and COX-2 (Fig. 9E). To further demonstrate that PPARβ is activated by HGF-induced COX-2 expression, transactivation studies were done with reporter constructs containing PPREs from the *PDK1* and *ILK* genes (10). As shown in Fig. 9F, HGF increased the luciferase activity through these PPREs by ~2-fold. Interestingly, this reporter activation was blocked by the COX-2 inhibitor, suggesting that HGF-mediated PPARβ activation in HF keratinocytes is dependent on COX-2.

Altogether, these results demonstrate that HGF activates PPARβ in a COX-2-dependent manner in keratinocytes, which in turn stimulates the Akt1 pathway through up-regulation of its two target genes *PDK1* and *ILK*. This pathway finally protects hair pegs from premature apoptosis during early HF morphogenesis, thus allowing for normal HF development (Fig. 10).

DISCUSSION

The results herein show that PPARβ and Akt1 are highly expressed in follicular keratinocytes throughout the whole process of HF morphogenesis, from hair placodes to mature HFs (Fig. 10B). Interestingly, deletion of PPARβ in mice is associated with a significant retardation in HF development specifically from the hair peg stage, mainly due to premature increased apoptosis of follicular keratinocytes. The antiapoptotic function of PPARβ is mediated via a temporally coordinated activation of the Akt1 signaling pathway in developing HFs, revealing a new important function of Akt1 in the maturation of hair pegs. Most importantly, we show that mesenchyme-secreted HGF is a likely signal that leads to the timely activation of PPARβ in early HFs, via the induction of COX-2 expression, and hence production of PPARβ ligands (Fig. 10C). Unlike proinflammatory stimuli which up-regulate both the expression of PPARβ and production of its ligands (41), epithelium-mesenchyme interactions appear to be involved only in the latter, which leads to ligand-dependent activation of PPARβ already present at high levels.

PPARβ is a nuclear receptor with a novel function in hair follicle development. Several members of the nuclear hormone receptor family have been identified as important modulators of skin and HF development and homeostasis. The well-studied nuclear receptors in HFs are the vitamin D and retinoid receptors (1). However, thyroid and glucocorticoid hormones have also been shown to affect hair growth in rodents and humans. Herein, we identified PPARβ as an additional nuclear receptor regulating HF development. Interestingly, conditional deletion in the skin of RXRα, the most abundant heterodimeric partner of PPARs in keratinocytes, resulted in a similar delay in postnatal HF development, supporting the participation of PPARβ and RXRα heterodimers in the regulation of HF morphogenesis (23). In the same report, RXRα was also found to regulate the initiation of the anagen phase during HF cycling, as a heterodimer of the vitamin D receptor. However, according to the role of PPARβ during HF morphogenesis, one cannot exclude that PPARβ may also be involved in HF cycling. In support of this, many growth modulators that regulate HF development have also been shown to control the cyclic activity of postnatal HFs.

The antiapoptotic role of PPARβ contributes to efficient hair follicle development. The mammalian HF is a complex organ that comprises several cell types from various embryo-

Akt1 in the presence of the Akt inhibitor was observed by using immunofluorescence staining (right panel). (B) Longitudinal cryosections of four different PPARβ$^{+/+}$ and PPARβ$^{-/-}$ skin explants treated (Akt inhibitor) with the Akt inhibitor or not treated (vehicle) were stained for endogenous alkaline phosphatase activity as a marker for the developing dermal papilla and counterstained with hematoxylin-eosin (left top panels). The hair scores (left bottom panel) and the percentages of HFs at distinct stages of morphogenesis (right panel) were determined by quantitative histomorphometry. (C) Representative staining for PCNA (proliferation marker) and TUNEL (apoptotic marker) in PPARβ$^{+/+}$ skin explants treated (Akt inhibitor) with the Akt inhibitor or not treated (vehicle) are given (right panel). Percentages of PCNA- and TUNEL-positive cells were quantified among the population of follicular keratinocytes localized in early HFs (stages 1 to 4; left panel). Independent Student's *t* test: *, $P < 0.05$; **, $P < 0.01$. Magnification bars, 50 μm.

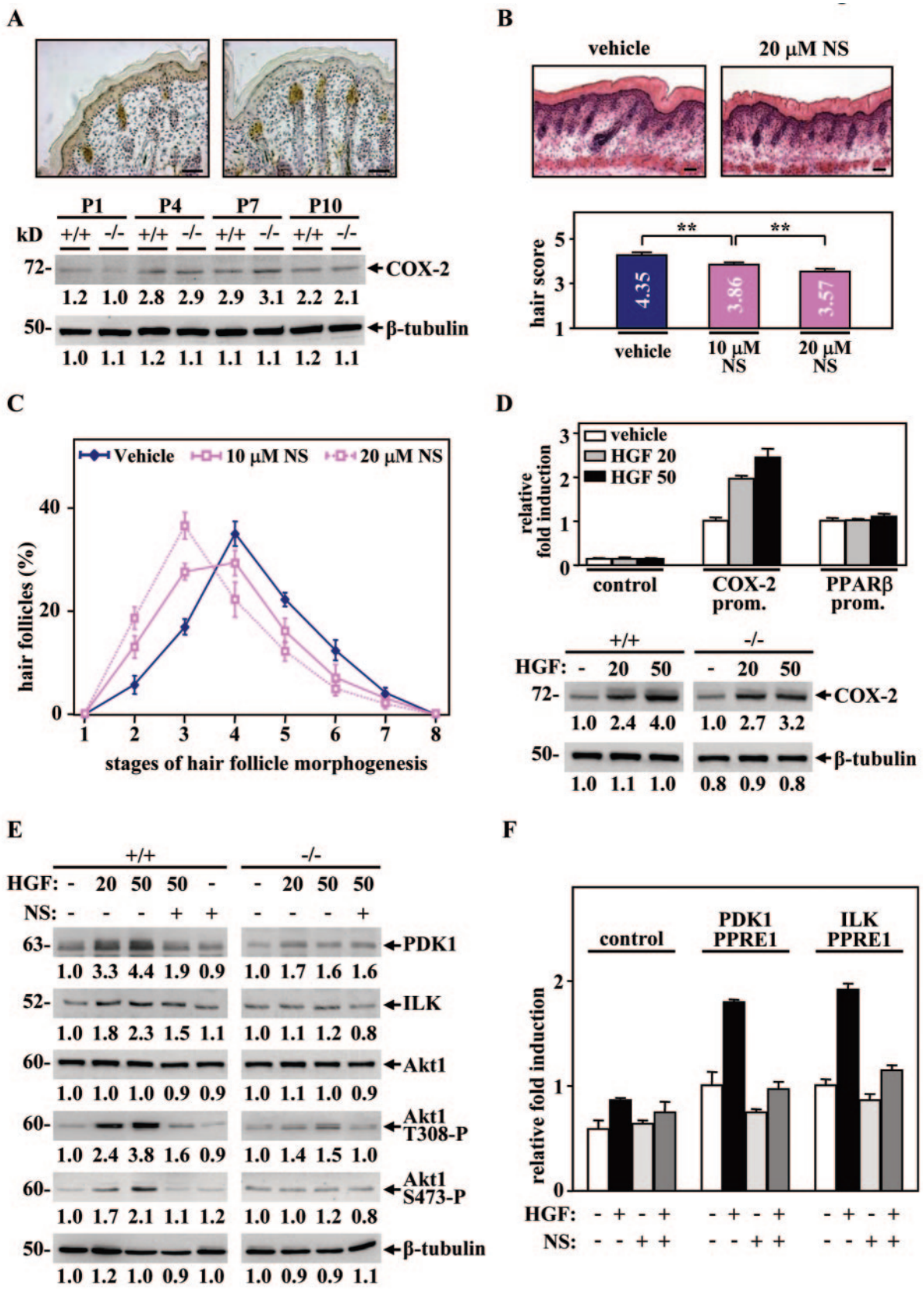

FIG. 9. HGF-mediated activation of PPARβ is dependent on COX-2 activity. (A) Colorimetric immunostaining of COX-2 in hair pegs and mature HFs was performed in WT mouse skin at P4 (top panel). Analysis of COX-2 protein expression was carried out at indicated postnatal days. (B, C) Quantitative histomorphometry was done on four different skin explants treated or not for 48 h with 10 or 20 μM of the COX-2 inhibitor

logical origins, keratinocytes, melanocytes, and specialized fibroblasts (dermal papilla cells). Like other ectodermal derivates, HF development in embryonic skin is governed by epithelium-mesenchyme interactions (31). Following HF induction (first dermal signal), HF precursors emerge first as placodes in the uniform epithelium surface. Once placodes form, epithelial signals pass from the placodes to the underlying dermis, causing the clustering of a group of cells (mesenchymal condensation) that will form the dermal papilla. A second dermal signal from the dermal condensate to the follicular epithelium directs the proliferation and downgrowth of epithelial cells (hair pegs) into the dermis. Finally, cell differentiation in the developing HF leads to the formation of the typical structures of mature HFs, like root sheaths, hair matrix, hair shafts, and sebocytes (Fig. 10A).

Analysis of PPARβ expression during murine HF morphogenesis revealed its specific expression in the epithelial compartment at early stages of development, from hair placodes to hair pegs (stages 1 to 4). From stage 5, PPARβ expression progressively disappears from the interfollicular epidermis, as previously described (29), and becomes restricted to ORS and matrix cells of mature HFs (Fig. 10B). A similar expression pattern was reported in the epithelial compartment of human anagen HFs, although PPAR expression was also located in dermal papilla cells (3). We demonstrate here that deletion of PPARβ in mice leads to a significant transient retardation in HF morphogenesis, associated with a thinner subcutaneous fat layer in newborn mice. Interestingly, the latter phenotype was also described in PPARβ-null adult mice (2). Despite the early expression of PPARβ in the epithelial HF precursors, HF development initiates correctly in PPARβ-null animals, suggesting that the initial signaling events (epidermal thickening and dermal papilla formation) in folliculogenesis are independent of PPARβ. However, subsequent hair peg elongation into the dermis was delayed, as a consequence of premature increased apoptosis in follicular keratinocytes of PPARβ-deficient skin. Interestingly, delayed HF morphogenesis resulting from aberrant apoptosis in keratinocytes was previously reported in E2F1-transgenic mice (37) and in Noggin-knockout mice (4), emphasizing the importance of regulated apoptosis during HF development.

Importance of the Akt1 pathway in vivo during hair peg maturation. During HF morphogenesis, the elongation of hair pegs is largely due to proliferation of epidermal cells. Although little is known about the regulation of this growth, recent evidence suggests that SHH plays an important role. SHH is expressed in epidermal cells as they invaginate into the dermis, and developing HFs from SHH-null mice exhibit reduced proliferation and fail to progress beyond the hair germ stage (31). However, SHH expression and the proliferative index of hair pegs are only slightly altered in PPARβ$^{-/-}$ skin. In agreement with our earlier report on wound healing (10), we show that during HF morphogenesis, PPARβ activation protects the keratinocytes from apoptosis through activation of the Akt1 pathway. Indeed, active Akt1 precisely colocalizes with PPARβ in the epithelial compartment of growing HFs (Fig. 10B) and deletion of PPARβ or Akt1 in mice leads to a similar retardation in HF morphogenesis from the hair peg stage. This newly identified function of Akt1 during HF development is consistent with impaired HF morphogenesis at early stages recently observed in Akt1/2 DKO mice (36). It's interesting that the phenotype of these DKO mice appears more severe than single-gene deletion, suggesting partial redundancy of functions between the Akt family members in the skin. In agreement with the role of the phosphatidylinositol-3-kinase (PI3K)/Akt1 pathway in HF development, growth factor receptors that signal through PI3K, including the epidermal growth factor receptor, have already been strongly implicated in HF growth (15, 34). Most interestingly, keratinocyte-specific deletion of PTEN, a negative regulator of the PI3K/Akt pathway whose expression is repressed by PPARβ (11), resulted in accelerated HF morphogenesis in newborn mice (40). Furthermore, the deletion of the murine serum- and glucocorticoid-regulated kinase 3 (SGK-3), which is closely related to the Akt kinases, resulted in a defect in postnatal HF morphogenesis from P4 (28). Finally, no defect in HF growth could be reported in mice deficient of one of the Akt targets FKHR or GSK-3β, because of the embryonic lethality at early developmental stages of these deletions (13, 17). Interestingly, others have shown that the overexpression of a dominant-negative GSK-3β in mammary epithelium results in the transdifferentiation into hair follicle-like structures, which expressed high levels of hair-specific keratin markers (32).

Finally, adhesion and extracellular matrix molecules are known to regulate tissue morphogenesis and are necessary for normal follicular development. In accordance with a possible implication of PPARβ in cell adhesion and migration processes (10), it is tempting to make a parallel between the altered HF morphogenesis described upon deletion of β1-integrin (38) or laminin-10 (22) and our observations on delayed HF development in PPARβ-null mice, which occurs at similar stages.

NS-398 (NS). Delayed HF morphogenesis was observed in explants treated with NS-398, as reflected by the decrease of the hair morphogenesis score in a dose-dependent manner. Independent Student's *t* test: ∗, $P < 0.05$; ∗∗, $P < 0.01$. Magnification bars, 50 μm. (D) Mouse keratinocytes were transfected with a luciferase reporter construct with or without (control) the proximal promoter of the *COX-2* (COX-2 prom.) or *PPARβ* (PPARβ prom.) genes. The transfected cells were allowed to recover for 24 h and were then treated for another 24 h with 20 or 50 μM HGF (top panel) or not treated (vehicle). The relative *n*-fold induction in treated versus untreated cells was calculated after normalization to β-galactosidase activity. Values are means of at least three independent experiments. In the bottom panel, Western blot assays were carried out using total cellular proteins extracted from primary keratinocytes derived from PPARβ$^{+/+}$ and PPARβ$^{-/-}$ mice and treated for 24 h with 20 or 50 μM of HGF or not treated (−). (E) Analysis of the Akt1 pathway by Western blotting was performed in primary keratinocytes derived from PPARβ$^{+/+}$ and PPARβ$^{-/-}$ mice, treated for 24 h with 20 or 50 μM of HGF or not treated (−), in the absence (−) or presence (+) of 10 μM NS-398 (NS; left panel). Changes, indicated below each band, represent the mean of three independent experiments, after normalization to the untreated PPARβ$^{+/+}$ or PPARβ$^{-/-}$. (F) Mouse keratinocytes were transfected with luciferase reporter constructs containing or not containing (control) two copies of *ILK* or *PDK1* PPREs and treated (+) or not treated (−) with 20 μM HGF and/or 10 μM NS-398 (NS). Results represent means of three independent experiments and are expressed as relative *n*-fold induction.

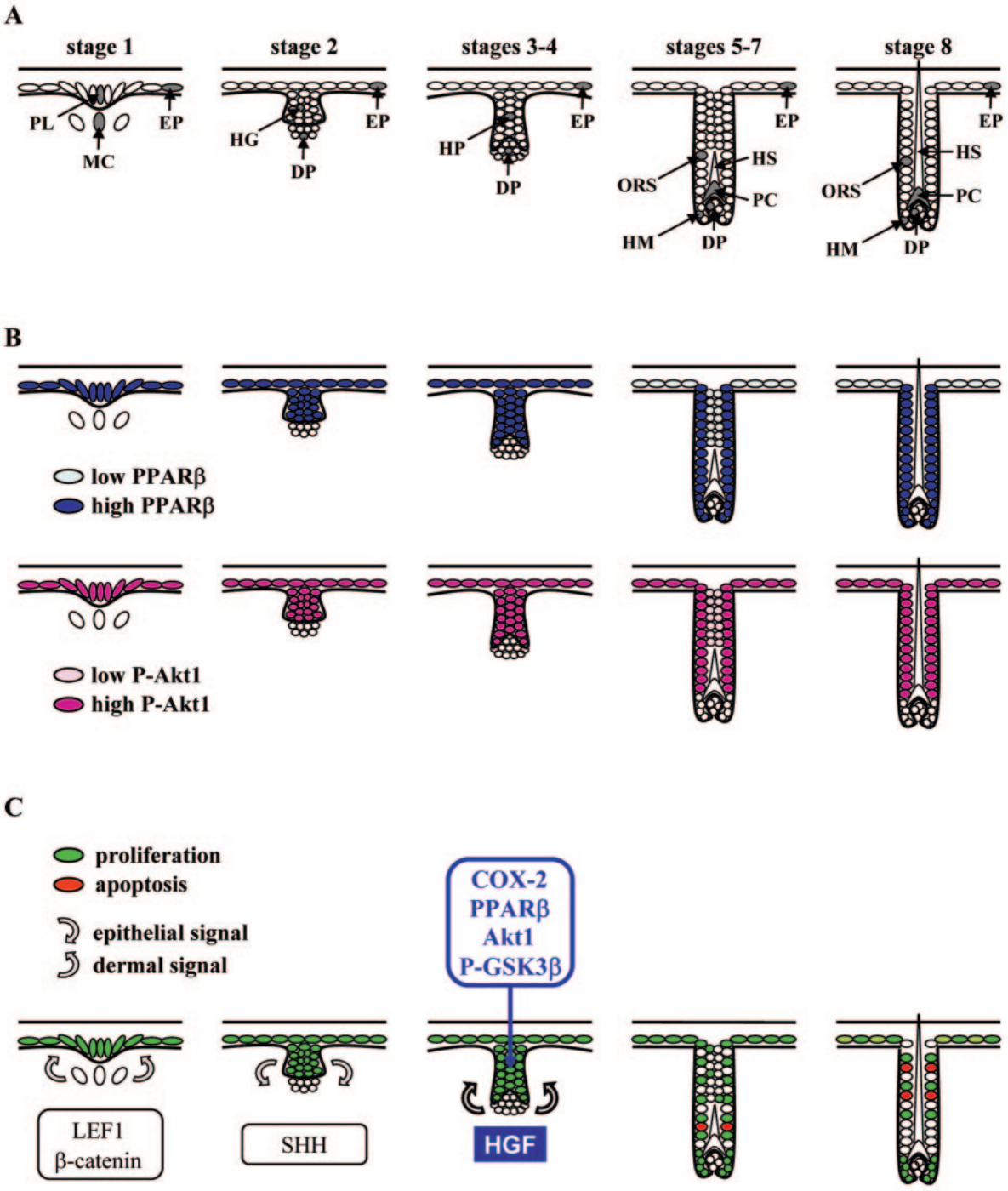

FIG. 10. Model for the anti-apoptotic role of PPARβ during hair follicle morphogenesis. (A) Schematic representation of murine HF development. The developmental stage of HF morphogenesis is indicated according to Paus et al. (35). EP, epidermis; PL, hair placode; MC, mesenchymal condensation; HG, hair germ; HP, hair peg; DP, dermal papilla; HM, hair matrix; PC, precortex; HS, hair shaft. (B) Summary of the distribution of PPARβ and phosphorylated Akt1 during HF development. Colocalization of both proteins was consecutively observed in the hair placode, hair germ, hair peg, and outer root sheath of the developing HF, whereas dermal papilla was negative. Differences in protein expression levels are reflected by color intensity. (C) Model for the role of PPARβ during HF development. The first two signals (gray arrows) leading consecutively to placode thickening (first dermal signal, stage 1) and dermal papilla formation (first epithelial signal, stage 2) are likely to involve β-catenin/LEF1 and SHH signaling pathways, respectively. The exact nature of the second dermal signal leading to hair peg elongation is not known, but it may involve HGF and its receptor Met, which are expressed in dermal condensate and hair peg, respectively. The paracrine factor HGF activates PPARβ in a COX-2-dependent manner in the proliferating hair pegs, leading to activation of the Akt1 signaling pathway and protection of follicular keratinocytes against premature apoptosis. Proliferative and apoptotic cells, as revealed by PCNA and TUNEL staining, are shown in green and red, respectively.

The activity of PPARβ in hair follicle keratinocytes requires COX-2 expression and HGF production. Distinct growth factors and prostaglandin types have been described as regulators of HF development and cycling in humans (19). In addition, the COX-2 enzyme, which catalyzes the formation of prostaglandins from arachidonic acid, was shown to affect HF growth in mice (21). Recently, COX-2 expression and activity have also been associated with early HF morphogenesis around the hair peg stage (33). In this report, transgenic COX-2 overexpression in the skin with the keratin 5 promoter induced a precocious entry of growing HFs into the first catagen stage after birth. However, it did not affect early HF morphogenesis, which is consistent with the late appearance of keratin 5 expression in the ORS of developing HFs. We demonstrate here that, in contrast, COX-2 activity is necessary for early HF development in organ culture. Most likely COX-2 acts through the production of ligands that stimulate PPARβ activity in follicular keratinocytes. Similar activation of PPARβ by COX-2 eicosanoid products has already been implicated in embryo implantation, colorectal cancer, and vascular functions (24). Another piece of evidence supporting the importance of COX-2 activity for PPARβ function in the skin is their overlapping expression patterns. Indeed, besides the colocalization of COX-2 and PPARβ in early HFs and embryonic interfollicular epidermis, they both disappear in normal adult epidermis and are rapidly reactivated following tetradecanoyl phorbol acetate application, skin wounding, hair plucking, or carcinogenesis (21, 29). In accordance with our observations on the antiapoptotic role of PPARβ, different COX-2-derived products, including PGI2 and PGE2 prostaglandins, were shown to increase cell survival in a PPARβ-dependent manner both in vitro and in vivo (8, 16, 43). Furthermore, COX-2 has also been reported to suppress apoptosis in lung cancer cells by activating the Akt-dependent pathway (25). However, it is also possible that other enzymes participate in PPARβ activation in elongating hair pegs. For example, lipoxygenases have also been located in early HFs (12) and lipoxygenase-derived eicosanoids were shown to activate PPARβ in human keratinocytes (44). Nevertheless, the fact that the COX-2 inhibitor affects HF maturation underscores the importance of COX-2-controlled ligand production in PPARβ activation during HF growth.

We reveal here that HGF, which is produced by dermal papilla cells during early HF development, induces COX-2 expression in keratinocytes, leading to the activation of PPARβ and subsequent stimulation of the Akt1 pathway at a specific stage of HF development (Fig. 10C). However, in contrast to tumor necrosis factor alpha, or other inflammatory cytokines that regulate both PPARβ expression and activation, the role of HGF seems restricted to PPARβ activation. HGF is a versatile modulator of cell proliferation, migration, differentiation and apoptosis, and has been implicated in the control of epithelium-mesenchyme interactions in a wide range of mammalian tissues. In addition to HF development, an important role of HGF was also attributed in the morphogenesis of other ectodermal derivates such as teeth, feather and mammary glands, and may therefore also require PPARβ activity. In addition, the ability of HGF to indirectly modulate PPARβ activity may have significant impact on other processes where both proteins have been involved, like placental organogenesis (10, 42) and tissue wound healing (18, 29).

Altogether, this work demonstrates that epithelium-mesenchyme interactions control PPARβ functions by modulating its activity during HF morphogenesis, and increases our current knowledge of molecular signaling pathways involved in the control of HF growth.

ACKNOWLEDGMENTS

We thank Véronique Borel, Vincent Roh, and Debby Hynx for valuable technical help and A. Delgado for critical reading of the manuscript.

This work was supported by the Swiss National Science Foundation (grants to Walter Wahli and to Béatrice Desvergne) and by the Etat de Vaud. The Friedrich Miescher Institute for biomedical research is supported by the Novartis research foundation.

REFERENCES

1. **Alonso, L. C., and R. L. Rosenfield.** 2003. Molecular genetic and endocrine mechanisms of hair growth. Horm. Res. **60:**1–13.
2. **Barak, Y., D. Liao, W. He, E. S. Ong, M. C. Nelson, J. M. Olefsky, R. Boland, and R. M. Evans.** 2002. Effects of peroxisome proliferator-activated receptor delta on placentation, adiposity, and colorectal cancer. Proc. Natl. Acad. Sci. USA **99:**303–308.
3. **Billoni, N., B. Buan, B. Gautier, C. Collin, O. Gaillard, Y. F. Mahe, and B. A. Bernard.** 2000. Expression of peroxisome proliferator activated receptors (PPARs) in human hair follicles and PPAR alpha involvement in hair growth. Acta Derm. Venereol. **80:**329–334.
4. **Botchkarev, V. A., N. V. Botchkareva, W. Roth, M. Nakamura, L. H. Chen, W. Herzog, G. Lindner, J. A. McMahon, C. Peters, R. Lauster, A. P. McMahon, and R. Paus.** 1999. Noggin is a mesenchymally derived stimulator of hair-follicle induction. Nat. Cell Biol. **1:**158–164.
5. **Braissant, O., and W. Wahli.** 1998. Differential expression of peroxisome proliferator-activated receptor-alpha, -beta, and -gamma during rat embryonic development. Endocrinology **139:**2748–2754.
6. **Brazil, D. P., Z. Z. Yang, and B. A. Hemmings.** 2004. Advances in protein kinase B signalling: AKTion on multiple fronts. Trends Biochem. Sci. **29:** 233–242.
7. **Castillo, S. S., J. Brognard, P. A. Petukhov, C. Zhang, J. Tsurutani, C. A. Granville, M. Li, M. Jung, K. A. West, J. G. Gills, A. P. Kozikowski, and P. A. Dennis.** 2004. Preferential inhibition of Akt and killing of Akt-dependent cancer cells by rationally designed phosphatidylinositol ether lipid analogues. Cancer Res. **64:**2782–2792.
8. **Cutler, N. S., R. Graves-Deal, B. J. LaFleur, Z. Gao, B. M. Boman, R. H. Whitehead, E. Terry, J. D. Morrow, and R. J. Coffey.** 2003. Stromal production of prostacyclin confers an antiapoptotic effect to colonic epithelial cells. Cancer Res. **63:**1748–1751.
9. **Desvergne, B., and W. Wahli.** 1999. Peroxisome proliferator-activated receptors: nuclear control of metabolism. Endocr. Rev. **20:**649–688.
10. **Di Poi, N., L. Michalik, N. S. Tan, B. Desvergne, and W. Wahli.** 2003. The anti-apoptotic role of PPARbeta contributes to efficient skin wound healing. J. Steroid Biochem. Mol. Biol. **85:**257–265.
11. **Di Poi, N., N. S. Tan, L. Michalik, W. Wahli, and B. Desvergne.** 2002. Antiapoptotic role of PPARbeta in keratinocytes via transcriptional control of the Akt1 signaling pathway. Mol. Cell **10:**721–733.
12. **Funk, C. D., D. S. Keeney, E. H. Oliw, W. E. Boeglin, and A. R. Brash.** 1996. Functional expression and cellular localization of a mouse epidermal lipoxygenase. J. Biol. Chem. **271:**23338–23344.
13. **Furuyama, T., K. Kitayama, Y. Shimoda, M. Ogawa, K. Sone, K. Yoshida-Araki, H. Hisatsune, S. Nishikawa, K. Nakayama, K. Nakayama, K. Ikeda, N. Motoyama, and N. Mori.** 2004. Abnormal angiogenesis in Foxo1 (Fkhr)-deficient mice. J. Biol. Chem. **279:**34741–34749.
14. **Hager, B., J. R. Bickenbach, and P. Fleckman.** 1999. Long-term culture of murine epidermal keratinocytes. J. Investig. Dermatol. **112:**971–976.
15. **Hansen, L. A., N. Alexander, M. E. Hogan, J. P. Sundberg, A. Dlugosz, D. W. Threadgill, T. Magnuson, and S. H. Yuspa.** 1997. Genetically null mice reveal a central role for epidermal growth factor receptor in the differentiation of the hair follicle and normal hair development. Am. J. Pathol. **150:**1959–1975.
16. **Hao, C. M., R. Redha, J. Morrow, and M. D. Breyer.** 2002. Peroxisome proliferator-activated receptor delta activation promotes cell survival following hypertonic stress. J. Biol. Chem. **277:**21341–21345.
17. **Hoeflich, K. P., J. Luo, E. A. Rubie, M. S. Tsao, O. Jin, and J. R. Woodgett.** 2000. Requirement for glycogen synthase kinase-3beta in cell survival and NF-kappaB activation. Nature **406:**86–90.
18. **Huh, C. G., V. M. Factor, A. Sanchez, K. Uchida, E. A. Conner, and S. S. Thorgeirsson.** 2004. Hepatocyte growth factor/c-met signaling pathway is

required for efficient liver regeneration and repair. Proc. Natl. Acad. Sci. USA **101:**4477–4482.
19. **Johnstone, M. A., and D. M. Albert.** 2002. Prostaglandin-induced hair growth. Surv. Ophthalmol. **47**(Suppl. 1)**:**S185–S202.
20. **Kersten, S., B. Desvergne, and W. Wahli.** 2000. Roles of PPARs in health and disease. Nature **405:**421–424.
21. **Lee, J. L., H. Mukhtar, D. R. Bickers, L. Kopelovich, and M. Athar.** 2003. Cyclooxygenases in the skin: pharmacological and toxicological implications. Toxicol. Appl. Pharmacol. **192:**294–306.
22. **Li, J., J. Tzu, Y. Chen, Y. P. Zhang, N. T. Nguyen, J. Gao, M. Bradley, D. R. Keene, A. E. Oro, J. H. Miner, and M. P. Marinkovich.** 2003. Laminin-10 is crucial for hair morphogenesis. EMBO J. **22:**2400–2410.
23. **Li, M., H. Chiba, X. Warot, N. Messaddeq, C. Gerard, P. Chambon, and D. Metzger.** 2001. RXR-alpha ablation in skin keratinocytes results in alopecia and epidermal alterations. Development **128:**675–688.
24. **Lim, H., and S. K. Dey.** 2002. A novel pathway of prostacyclin signaling-hanging out with nuclear receptors. Endocrinology **143:**3207–3210.
25. **Lin, M. T., R. C. Lee, P. C. Yang, F. M. Ho, and M. L. Kuo.** 2001. Cyclooxygenase-2 inducing Mcl-1-dependent survival mechanism in human lung adenocarcinoma CL1.0 cells. Involvement of phosphatidylinositol 3-kinase/Akt pathway. J. Biol. Chem. **276:**48997–49002.
26. **Lindner, G., A. Menrad, E. Gherardi, G. Merlino, P. Welker, B. Handjiski, B. Roloff, and R. Paus.** 2000. Involvement of hepatocyte growth factor/scatter factor and met receptor signaling in hair follicle morphogenesis and cycling. FASEB J. **14:**319–332.
27. **Magerl, M., D. J. Tobin, S. Muller-Rover, E. Hagen, G. Lindner, I. A. McKay, and R. Paus.** 2001. Patterns of proliferation and apoptosis during murine hair follicle morphogenesis. J. Investig. Dermatol. **116:**947–955.
28. **McCormick, J. A., Y. Feng, K. Dawson, M. J. Behne, B. Yu, J. Wang, A. W. Wyatt, G. Henke, F. Grahammer, T. M. Mauro, F. Lang, and D. Pearce.** 2004. Targeted disruption of the protein kinase SGK3/CISK impairs postnatal hair follicle development. Mol. Biol. Cell **15:**4278–4288.
29. **Michalik, L., B. Desvergne, N. S. Tan, S. Basu-Modak, P. Escher, J. Rieusset, J. M. Peters, G. Kaya, F. J. Gonzalez, J. Zakany, D. Metzger, P. Chambon, D. Duboule, and W. Wahli.** 2001. Impaired skin wound healing in peroxisome proliferator-activated receptor (PPAR)alpha and PPARbeta mutant mice. J. Cell Biol. **154:**799–814.
30. **Michalik, L., B. Desvergne, and W. Wahli.** 2004. Peroxisome-proliferator-activated receptors and cancers: complex stories. Nat. Rev. Cancer **4:**61–70.
31. **Millar, S. E.** 2002. Molecular mechanisms regulating hair follicle development. J. Investig. Dermatol. **118:**216–225.
32. **Miyoshi, K., A. Rosner, M. Nozawa, C. Byrd, F. Morgan, E. Landesman-Bollag, X. Xu, D. C. Seldin, E. V. Schmidt, M. M. Taketo, G. W. Robinson, R. D. Cardiff, and L. Hennighausen.** 2002. Activation of different Wnt/beta-catenin signaling components in mammary epithelium induces transdifferentiation and the formation of pilar tumors. Oncogene **21:**5548–5556.
33. **Muller-Decker, K., C. Leder, M. Neumann, G. Neufang, C. Bayerl, J. Schweizer, F. Marks, and G. Furstenberger.** 2003. Expression of cyclooxygenase isozymes during morphogenesis and cycling of pelage hair follicles in mouse skin: precocious onset of the first catagen phase and alopecia upon cyclooxygenase-2 overexpression. J. Investig. Dermatol. **121:**661–668.
34. **Murillas, R., F. Larcher, C. J. Conti, M. Santos, A. Ullrich, and J. L. Jorcano.** 1995. Expression of a dominant negative mutant of epidermal growth factor receptor in the epidermis of transgenic mice elicits striking alterations in hair follicle development and skin structure. EMBO J. **14:**5216–5223.
35. **Paus, R., S. Muller-Rover, C. Van Der Veen, M. Maurer, S. Eichmuller, G. Ling, U. Hofmann, K. Foitzik, L. Mecklenburg, and B. Handjiski.** 1999. A comprehensive guide for the recognition and classification of distinct stages of hair follicle morphogenesis. J. Investig. Dermatol. **113:**523–532.
36. **Peng, X. D., P. Z. Xu, M. L. Chen, A. Hahn-Windgassen, J. Skeen, J. Jacobs, D. Sundararajan, W. S. Chen, S. E. Crawford, K. G. Coleman, and N. Hay.** 2003. Dwarfism, impaired skin development, skeletal muscle atrophy, delayed bone development, and impeded adipogenesis in mice lacking Akt1 and Akt2. Genes Dev. **17:**1352–1365.
37. **Pierce, A. M., S. M. Fisher, C. J. Conti, and D. G. Johnson.** 1998. Deregulated expression of E2F1 induces hyperplasia and cooperates with ras in skin tumor development. Oncogene **16:**1267–1276.
38. **Raghavan, S., C. Bauer, G. Mundschau, Q. Li, and E. Fuchs.** 2000. Conditional ablation of beta1 integrin in skin. Severe defects in epidermal proliferation, basement membrane formation, and hair follicle invagination. J. Cell Biol. **150:**1149–1160.
39. **Rosenfield, R. L., D. Deplewski, and M. E. Greene.** 2000. Peroxisome proliferator-activated receptors and skin development. Horm. Res. **54:**269–274.
40. **Suzuki, A., S. Itami, M. Ohishi, K. Hamada, T. Inoue, N. Komazawa, H. Senoo, T. Sasaki, J. Takeda, M. Manabe, T. W. Mak, and T. Nakano.** 2003. Keratinocyte-specific Pten deficiency results in epidermal hyperplasia, accelerated hair follicle morphogenesis and tumor formation. Cancer Res. **63:**674–681.
41. **Tan, N. S., L. Michalik, N. Noy, R. Yasmin, C. Pacot, M. Heim, B. Fluhmann, B. Desvergne, and W. Wahli.** 2001. Critical roles of PPAR beta/delta in keratinocyte response to inflammation. Genes Dev. **15:**3263–3277.
42. **Uehara, Y., O. Minowa, C. Mori, K. Shiota, J. Kuno, T. Noda, and N. Kitamura.** 1995. Placental defect and embryonic lethality in mice lacking hepatocyte growth factor/scatter factor. Nature **373:**702–705.
43. **Wang, D., H. Wang, Q. Shi, S. Katkuri, W. Wahli, B. Desvergne, S. K. Das, S. K. Dey, and R. N. DuBois.** 2004. Prostaglandin E(2) promotes colorectal adenoma growth via transactivation of the nuclear peroxisome proliferator-activated receptor delta. Cancer Cell **6:**285–295.
44. **Westergaard, M., J. Henningsen, C. Johansen, S. Rasmussen, M. L. Svendsen, U. B. Jensen, H. D. Schroder, B. Staels, L. Iversen, L. Bolund, K. Kragballe, and K. Kristiansen.** 2003. Expression and localization of peroxisome proliferator-activated receptors and nuclear factor kappaB in normal and lesional psoriatic skin. J. Investig. Dermatol. **121:**1104–1117.
45. **Yang, Z. Z., O. Tschopp, M. Hemmings-Mieszczak, J. Feng, D. Brodbeck, E. Perentes, and B. A. Hemmings.** 2003. Protein kinase B alpha/Akt1 regulates placental development and fetal growth. J. Biol. Chem. **278:**32124–32131.
46. **Zeng, Q., L. K. McCauley, and C. Y. Wang.** 2002. Hepatocyte growth factor inhibits anoikis by induction of activator protein 1-dependent cyclooxygenase-2. Implication in head and neck squamous cell carcinoma progression. J. Biol. Chem. **277:**50137–50142.